

PLS-Assisted Offloading for Edge Computing-Enabled Post-Quantum Security in Resource-Constrained Devices

Hamid Amiriara, Mahtab Mirmohseni, and Rahim Tafazolli
Institute for Communication Systems, University of Surrey, Guildford, U.K.
 Email: {h.amiriara, m.mirmohseni, r.tafazolli}@surrey.ac.uk

Abstract—With the advent of post-quantum cryptography (PQC) standards, it has become imperative for resource-constrained devices (RCDs) in the Internet of Things (IoT) to adopt these quantum-resistant protocols. However, the high computational overhead and the large key sizes associated with PQC make direct deployment on such devices impractical. To address this challenge, we propose an edge computing-enabled PQC framework that leverages a physical-layer security (PLS)-assisted offloading strategy, allowing devices to either offload intensive cryptographic tasks to a post-quantum edge server (PQES) or perform them locally. Furthermore, to ensure data confidentiality within the edge domain, our framework integrates two PLS techniques: offloading RCDs employ wiretap coding to secure data transmission, while non-offloading RCDs serve as friendly jammers by broadcasting artificial noise to disrupt potential eavesdroppers. Accordingly, we co-design the computation offloading and PLS strategy by jointly optimizing the device transmit power, PQES computation resource allocation, and offloading decisions to minimize overall latency under resource constraints. Numerical results demonstrate significant latency reductions compared to baseline schemes, confirming the scalability and efficiency of our approach for secure PQC operations in IoT networks.

Index Terms—Post-quantum cryptography, edge computing, offloading, latency minimization, resource allocation.

I. INTRODUCTION

The Internet of Things (IoT) extends Internet connectivity to numerous embedded devices (e.g., sensors and actuators) and has seen rapid adoption in areas such as smart transportation, home automation, and e-healthcare [1]. Despite its advantages, securing these resource-constrained devices (RCDs) remains challenging due to their limited computing power, memory, and battery life. Such constraints complicate the deployment of modern cryptographic schemes, as these schemes often demand substantial computational resources [2].

Conventional cryptographic algorithms, such as Rivest–Shamir–Adleman (RSA) and elliptic curve cryptography (ECC), have secured digital systems for decades. However, quantum computing poses a critical threat as algorithms such as Shor’s can efficiently break these schemes [3]. To counter quantum threats, the National Institute of Standards and Technology (NIST) is standardizing post-quantum cryptography (PQC) algorithms, including Kyber, Dilithium, Falcon, and SPHINCS⁺ [4], [5]. However, these algorithms introduce new challenges for RCDs due to their high computational demands, large key sizes, and significant energy costs. To better illustrate these challenges, Table I compares these schemes to classical cryptography in terms of key sizes, ciphertext/signature sizes, and computational overhead. As shown in Table I, even at its lowest security

level (Dilithium-2), Dilithium requires a 1312-byte public key and a 2420-byte signature, approximately five and nine times larger than RSA, respectively. Meanwhile, SPHINCS⁺ has compact keys, but uses hash-based signing operations with extremely high CPU cycles per bit, and Falcon requires floating-point operations unsuitable for many IoT platforms.

A promising strategy for addressing these challenges is to offload computations to more capable edge nodes, thereby alleviating on-device overhead [9], [10]. While offloading PQC-related tasks can reduce resource consumption and enhance performance, transmitting sensitive data over wireless links exposes RCDs to eavesdroppers (EVEs). Conventional encryption-based approaches may still be susceptible to quantum attacks [11], and often require an RCD to encrypt data, which then must be decrypted and re-encrypted at the edge—greatly increasing computational complexity and latency.

Alternatively, physical-layer security (PLS) techniques, including wiretap coding and friendly jamming, can provide information-theoretic security directly over the wireless medium [12], [13]. Despite this potential, integrating PLS into an offloading framework requires a co-design approach that addresses both RCD constraints and limited network resources.

In this paper, we propose a PLS-assisted offloading scheme tailored to PQC in IoT networks. To reduce device-side overhead, the proposed framework allows each RCD to either process cryptographic tasks locally (as a non-offloading RCD) or offload them to a post-quantum edge server (PQES) (as an offloading RCD). To protect offloaded data, we integrate two PLS techniques: Offloading RCDs use wiretap coding for secure transmission, while non-offloading RCDs act as

TABLE I
 COMPARISON OF KEY SIZES, CIPHERTEXT (CT)/SIGNATURE (SIG) SIZES (IN BYTES), AND CPU-CYCLE OVERHEAD FOR CONVENTIONAL CRYPTOGRAPHIC AND PQC ALGORITHMS.

Algorithm	Security level	Pub. key	Priv. key	Ct/Sig	CPU* cycles/bit
RSA-2048	NA	256	256	256	113
ECC-256	NA	64	32	256	281
Kyber-512	1	800	1,632	768	2,193
Kyber-768	3	1,184	2,400	1,088	3,577
Kyber-1024	5	1,568	3,264	1,568	5,499
Dilithium-2	1	1,312	2,528	2,420	24,051
Dilithium-3	3	1,952	4,000	3,293	36,287
Dilithium-5	5	2,592	4,864	4,595	33,085
Falcon-512	1	897	1,281	690	148,791
Falcon-1024	3	1,793	2,305	1,330	326,105
SPHINCS ⁺ -128f	1	32	64	17,088	2,038,919
SPHINCS ⁺ -192f	3	48	96	35,664	2,686,303
SPHINCS ⁺ -256f	5	64	128	49,856	6,070,970

* CPU cycles/bit measured on ARM Cortex-M4 for encryption or signing of a 256-bit message, averaged over multiple runs [6]–[8].

friendly jammers by broadcasting artificial noise to degrade EVE's reception. Accordingly, we formulate a joint computation offloading and PLS co-design problem to minimize total latency by jointly optimizing transmit power (for offloading or jamming), computation resource allocation at the PQES, and the offloading decisions under transmit-power and computing-resource constraints.

The main contributions of this paper are outlined as follows:

- We introduce a PLS-assisted offloading framework for PQC in IoT that not only alleviates the computational load on RCDs but also secures offloaded data.
- We formulate a mixed-integer non-convex optimization problem aimed at minimizing the total latency across all RCDs by jointly optimizing RCD transmit power (for offloading/jamming), PQES computation resource allocation, and the offloading mode decisions. To solve this complex problem, we employ a variable separation and alternating optimization (AO) approach combined with successive convex approximation (SCA).
- To capture practical PQC-induced latency, our framework assigns CPU cycles per bit from Table I, accounting for varying PQC algorithms and security levels across RCDs.
- Through extensive simulations, we demonstrate that our proposed framework achieves significant latency reduction while maintaining robust security in PQC-enabled IoT deployments.

II. SYSTEM MODEL AND PROBLEM FORMULATION

A. System Model

As illustrated in Fig. 1, we consider an edge computing-enabled PQC system comprising a single PQES and K RCDs, under the threat of a malicious EVE.

Offloading and Jamming Strategy: Each RCD can operate in one of two modes: (i) As an *offloading RCD*, it offloads computationally intensive PQC tasks to the PQES. (ii) As a *non-offloading/jamming RCD*, it processes these tasks locally while simultaneously acting as a friendly jammer by broadcasting artificial noise. The mode selection for the k -th RCD is indicated by a binary variable α_k , where $\alpha_k = 1$ represents an offloading RCD and $\alpha_k = 0$ denotes a non-offloading RCD. Accordingly, the set of offloading RCDs is $\mathcal{K}_{\text{Off}} = \{k \mid \alpha_k = 1, k \in \mathcal{K}\}$, and the set of non-offloading RCDs is $\mathcal{K}_{\text{Non-off}} = \{k \mid \alpha_k = 0, k \in \mathcal{K}\}$, where $\mathcal{K} \triangleq \{1, 2, \dots, K\}$.

In this framework, the PQES allocates computing resources to efficiently process cryptographic tasks offloaded by devices in \mathcal{K}_{Off} , while devices in $\mathcal{K}_{\text{Non-off}}$ perform PQC locally and enhance security by transmitting artificial noise to jam potential EVE. Specifically, offloading RCDs use their transmit power $p_k, k \in \mathcal{K}_{\text{Off}}$ to send tasks to the PQES, whereas non-offloading RCDs use $p_k, k \in \mathcal{K}_{\text{Non-off}}$ to transmit jamming signals. This co-designed approach ensures that all RCDs contribute to both computational efficiency and data confidentiality.

Edge Computing Offloading Model: Let d_k denote the data size (in bits) of the data that must undergo cryptographic operation for the k -th RCD. Furthermore, let c_k represent the number of CPU cycles required per bit of data, which is determined by the specific PQC algorithm and the security level required by the k -th RCD (see Column 6 of Table I).

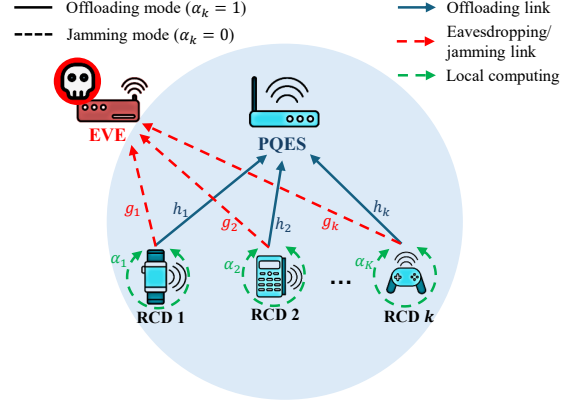


Fig. 1. PLS-assisted offloading in edge computing-enabled PQC systems.

1) *Local Computing:* Define f_0 as the local computing capacity (in CPU cycles per second) of each RCD. If the k -th RCD performs cryptographic processing locally, the corresponding local computing latency is given by [14],

$$T_k^{\text{Loc}} = \frac{d_k c_k}{f_0}, \quad \forall k \in \mathcal{K}_{\text{Non-off}}. \quad (1)$$

2) *Offloading to PQES:* For RCDs opting to offload, secure communication is enforced via wiretap coding and friendly jamming. The offloading rate for each RCD is defined as its achievable secrecy rate to the PQES, denoted as SR_k , ensuring the confidentiality of the data. Consequently, the transmission latency for the k -th RCD is expressed as,

$$T_k^{\text{Tra}} = \frac{d_k}{B SR_k}, \quad \forall k \in \mathcal{K}_{\text{Off}}, \quad (2)$$

where B is the available communication bandwidth. Let f_k represent the computational capacity allocated by the PQES to the k -th RCD. The computing latency at the PQES is then given by:

$$T_k^{\text{Off}} = \frac{d_k c_k}{f_k}, \quad \forall k \in \mathcal{K}_{\text{Off}}. \quad (3)$$

3) *Total Latency:* The overall latency for the k -th RCD's cryptographic task is thus:

$$T_k^{\text{Tot}} = (1 - \alpha_k) T_k^{\text{Loc}} + \alpha_k (T_k^{\text{Tra}} + T_k^{\text{Off}}), \quad \forall k \in \mathcal{K}. \quad (4)$$

Secure Communication Model: We denote h_k and g_k as the respective channel gains from the k -th RCD to the PQES and to EVE. We assume that the PQES has perfect knowledge of the RCD's channel state information (CSI), i.e., h_k , and their computational requirements. However, the PQES has only partial knowledge of EVE's CSI, denoted by g_k . Following the standard practice in PLS literature [15], we adopt a deterministic uncertainty model for EVE's CSI given by $g_k = \tilde{g}_k + \Delta g_k$, where \tilde{g}_k is the estimated channel gain for EVE, Δg_k is the estimation error, and $|\Delta g_k| \leq \epsilon$, with $\epsilon \geq 0$ representing the maximum possible estimation error.

In PLS, the worst-case secrecy rate (bits/sec/Hz) for the k -th RCD under a wiretap coding strategy is:

$$SR_k = [R_k^{\text{RCD}} - \max_{|\Delta g_k| \leq \epsilon} R_k^{\text{EVE}}]^+, \quad \forall k \in \mathcal{K}_{\text{Off}}, \quad (5)$$

where $[x]^+ \triangleq \max\{0, x\}$. The terms R_k^{RCD} and R_k^{EVE} represent the data transmission rate for the k -th RCD to the PQES and the achievable data rate for EVE to wiretap the k -th RCD's information, respectively, defined as

$$R_k^{\text{RCD}} = \log_2\left(1 + \frac{p_k h_k}{\sum_{i \in \mathcal{K}, i \neq k} p_j h_j + \sigma_{\text{RCD}}^2}\right), \quad (6)$$

$$R_k^{\text{EVE}} = \log_2\left(1 + \frac{p_k g_k}{\sum_{j \in \mathcal{K}, j \neq k} p_j g_j + \sigma_{\text{EVE}}^2}\right), \quad (7)$$

with σ_{RCD}^2 and σ_{EVE}^2 denote the variance of the additive white Gaussian noise at the RCD and EVE, respectively.

B. Problem Formulation

Under this setup, we aim to minimize overall RCD latency by jointly optimizing the transmit power vector $\mathbf{p} \triangleq \{p_k, k \in \mathcal{K}\}$, computing capacity allocation vector $\mathbf{f} \triangleq \{f_k, k \in \mathcal{K}_{\text{Off}}\}$, and the offloading decisions vector $\boldsymbol{\alpha} \triangleq \{\alpha_k, k \in \mathcal{K}\}$. Thus, the joint optimization problem is formulated as

$$(\mathcal{P}) : \quad \text{Minimize}_{\mathbf{p}, \mathbf{f}, \boldsymbol{\alpha}} \quad \sum_{k \in \mathcal{K}} T_k^{\text{Tot}} \quad (8a)$$

$$\text{s.t.} \quad \sum_{k \in \mathcal{K}} \alpha_k f_k \leq f^{\text{Tot}}, \quad (8b)$$

$$p_k \leq p^{\text{Max}}, \quad \forall k \in \mathcal{K}, \quad (8c)$$

$$\alpha_k \in \{0, 1\}, \quad \forall k \in \mathcal{K}, \quad (8d)$$

where f^{Tot} is the total computing capacity of the PQES, and p^{Max} is the maximum transmit power for each RCD. Next, by introducing a vector of auxiliary variables $\mathbf{t}^{\text{Th}} \triangleq \{t_k^{\text{Th}}, k \in \mathcal{K}\}$, we can reformulate (\mathcal{P}) into an equivalent problem as

$$(\mathcal{P}.1) : \quad \text{Minimize}_{\mathbf{p}, \mathbf{f}, \boldsymbol{\alpha}, \mathbf{t}^{\text{Th}}} \quad \sum_{k \in \mathcal{K}} t_k^{\text{Th}} \quad (9a)$$

$$\text{s.t.} \quad T_k^{\text{Tot}} \leq t_k^{\text{Th}}, \quad \forall k \in \mathcal{K}, \quad (9b)$$

$$(8b), (8c), (8d),$$

where t_k^{Th} is the maximum allowable latency for k -th RCD.

Due to channel uncertainties that affect the secrecy rate in (5), constraint (9b) makes problem $(\mathcal{P}.1)$ difficult to solve directly. Hence, to gain analytical tractability, we introduce a conservative upper bound on the latency terms, defined as:

$$T_k^{\text{Tot,UB}} \triangleq (1 - \alpha_k) T_k^{\text{Loc}} + \alpha_k \left(\frac{d_k}{B SR_k^{\text{LB}}} + T_k^{\text{Off}} \right), \quad (10)$$

where SR_k^{LB} is a conservative lower bound on the worst-case secrecy rate, defined as

$$SR_k^{\text{LB}} \triangleq [R_k^{\text{RCD}} - R_k^{\text{EVE,UB}}]^+, \quad \forall k \in \mathcal{K}, \quad (11)$$

and

$$R_k^{\text{EVE,UB}} = \log_2\left(1 + \frac{p_k g_k^+}{\sum_{j \in \mathcal{K}, j \neq k} p_j g_j^- + \sigma^2}\right), \quad (12)$$

where $g_k^+ = g_k + \epsilon$ and $g_j^- = g_j - \epsilon$ denote, respectively, the best- and worst-case channel gains for EVE from the PQES's perspective. With these modifications, problem $(\mathcal{P}.1)$ is reformulated as:

$$(\mathcal{P}.2) : \quad \text{Minimize}_{\mathbf{p}, \mathbf{f}, \boldsymbol{\alpha}, \mathbf{t}^{\text{Th}}} \quad \sum_{k \in \mathcal{K}} t_k^{\text{Th}} \quad (13a)$$

$$\text{s.t.} \quad T_k^{\text{Tot,UB}} \leq t_k^{\text{Th}}, \quad \forall k \in \mathcal{K}, \quad (13b)$$

$$(8b), (8c), (8d).$$

By enforcing $T_k^{\text{Tot,UB}} \leq t_k^{\text{Th}}$ in (13b), we ensure that the actual latency T_k^{Tot} also remains below t_k^{Th} despite channel estimation uncertainties, thereby maintaining the robustness and validity of constraint (9b).

III. PROPOSED SOLUTION

Problem $(\mathcal{P}.2)$ is inherently mixed-integer non-convex, making it challenging to find a globally optimal solution through standard methods. To address this, we propose a three-step AO algorithm. Specifically, we solve $(\mathcal{P}.2)$ by alternately optimizing the RCDs' transmit power p_k , computing capacity allocation f_k , and binary offloading decision variables α_k .

A. Sub-problem 1: RCDs' Transmit Power Optimization

With fixed computing capacity allocation f_k and offloading decision vector $\boldsymbol{\alpha}_k$, sub-problem 1 is defined as

$$(\mathcal{SP}1) : \quad \text{Minimize}_{\mathbf{p}, \mathbf{t}^{\text{Th}}} \quad \sum_{k \in \mathcal{K}} t_k^{\text{Th}} \quad (14a)$$

$$\text{s.t.} \quad SR_k^{\text{LB}} \geq \frac{d_k}{B(t_k^{\text{Th}} - T_k^{\text{Off}})}, \quad \forall k \in \mathcal{K}_{\text{Off}}, \quad (14b)$$

$$(8c).$$

Due to the non-concavity of R_k^{RCD} and non-convexity of $R_k^{\text{EVE,UB}}$, $(\mathcal{SP}1)$ is non-convex. To address this issue, first, we express the RCD rate R_k^{RCD} as the difference of two concave functions with respect to the transmit power vector \mathbf{p} :

$$R_k^{\text{RCD}} = I(\mathbf{p}) - J_k(\mathbf{p}), \quad (15)$$

where $I(\mathbf{p}) \triangleq \log_2(\sum_{k \in \mathcal{K}} p_k h_k + \sigma^2)$, and $J_k(\mathbf{p}) \triangleq \log_2(\sum_{j \in \mathcal{K}, j \neq k} p_j h_j + \sigma^2)$. The non-concavity of R_k^{RCD} arises from $J_k(\mathbf{p})$. To handle this, we employ the SCA approach. Specifically, in the r -th iteration of the SCA algorithm, $J_k(\mathbf{p})$ can be upper-bounded by:

$$\hat{J}_k^{(r)}(\mathbf{p}) \triangleq J_k(\mathbf{p}^{(r)}) + \frac{\sum_{i \in \mathcal{K}, i \neq k} (p_i - p_i^{(r)}) h_i}{\ln 2 (\sum_{i \in \mathcal{K}, i \neq k} p_i^{(r)} h_i + \sigma^2)}, \quad (16)$$

which is the first-order Taylor expansion of $J_k(\mathbf{p})$ around the local solution $\mathbf{p}^{(r)}$. Similarly, the upper bound on EVE's achievable rate is expressed as

$$R_k^{\text{EVE,UB}} = S_k(\mathbf{p}) - W_k(\mathbf{p}), \quad (17)$$

with $S_k(\mathbf{p}) \triangleq \log_2(p_k g_k^+ + \sum_{i \in \mathcal{K}, i \neq k} p_i g_i^- + \sigma^2)$, and $W_k(\mathbf{p}) \triangleq \log_2(\sum_{i \in \mathcal{K}, i \neq k} p_i g_i^- + \sigma^2)$. The non-convexity of $R_k^{\text{EVE,UB}}$ stems from $S_k(\mathbf{p})$. Accordingly, we approximate $S_k(\mathbf{p})$ via its first-order Taylor expansion:

$$\hat{S}_k^{(r)}(\mathbf{p}) \triangleq S_k(\mathbf{p}^{(r)}) + \frac{(p_k - p_k^{(r)}) g_k^+ + \sum_{i \in \mathcal{K}, i \neq k} (p_i - p_i^{(r)}) g_i^-}{\ln 2 (p_k^{(r)} g_k^+ + \sum_{i \in \mathcal{K}, i \neq k} p_i^{(r)} g_i^- + \sigma^2)}. \quad (18)$$

By replacing $J_k(\mathbf{p})$ with $\hat{J}_k^{(r)}(\mathbf{p})$ and $S_k(\mathbf{p})$ with $\hat{S}_k^{(r)}(\mathbf{p})$ in $(\mathcal{SP}1)$, we obtain the following convex approximation at the r -th iteration of the SCA:

$$(\mathcal{SP}1.r) : \quad \text{Minimize}_{\mathbf{p}, \mathbf{t}^{\text{Th}}} \quad \sum_{k \in \mathcal{K}} t_k^{\text{Th}} \quad (19a)$$

$$\text{s.t.} \quad I(\mathbf{p}) - \hat{J}_k^{(r)}(\mathbf{p}) - \hat{S}_k^{(r)}(\mathbf{p}) + \quad (19b)$$

$$W_k(\mathbf{p}) \geq \frac{d_k}{B(t_k^{\text{Th}} - T_k^{\text{Off}})}, \quad \forall k \in \mathcal{K}_{\text{Off}},$$

$$(8c).$$

This convex problem can then be solved optimally using convex solvers such as CVX.

Algorithm 1 Proposed AO-SCA Algorithm for Problem (\mathcal{P})

- 1: **Initialize:** feasible $\mathbf{p}^{(0)}$, $\mathbf{f}^{(0)}$, and $\boldsymbol{\alpha}^{(0)}$, iteration index $r \leftarrow 0$.
- 2: **repeat**
- 3: **Step 1:** Solve ($\mathcal{SP1.r}$) using the current $\mathbf{f}^{(r)}$ and $\boldsymbol{\alpha}^{(r)}$ to update $\mathbf{p}^{(r+1)}$.
- 4: **Step 2:** Update $\mathbf{f}^{(r+1)}$ via (21), using $\mathbf{p}^{(r+1)}$ and $\boldsymbol{\alpha}^{(r)}$.
- 5: **Step 3:** Solve relaxed ($\mathcal{SP3}$) and apply greedy rounding to update $\boldsymbol{\alpha}^{(r+1)}$.
- 6: $r \leftarrow r + 1$
- 7: **until** the change in objective value falls below the threshold δ_{AO} .

B. Sub-problem 2: Computing Capacity Allocation

Given fixed α_k and p_k , the sub-problem of computing capacity allocation derived from (\mathcal{P}) can be simplified as:

$$\begin{aligned} (\mathcal{SP2}) : \quad & \underset{\mathbf{f}}{\text{Minimize}} \quad \sum_{k \in \mathcal{K}} T_k^{\text{Off}} & (20a) \\ & \text{s.t.} \quad (8b). \end{aligned}$$

This strictly convex problem admits a unique optimal solution via the Karush–Kuhn–Tucker (KKT) conditions. The Lagrangian is $\mathcal{L} = \sum_k \frac{d_k c_k}{f_k} + \lambda(\sum_k f_k - f^{\text{Tot}})$, and the stationarity condition gives $f_k^* = \sqrt{d_k c_k / \lambda}$. Substituting this into the constraint (8b) yields the optimal allocation:

$$f_k^* = \frac{\sqrt{d_k c_k}}{\sum_{j \in \mathcal{K}} \sqrt{d_j c_j}} f^{\text{Tot}}. \quad (21)$$

C. Sub-problem 3: Offloading Decision Optimization

with fixed values of f_k and p_k , problem (\mathcal{P}) reduces to optimizing only the binary offloading decision vector:

$$\begin{aligned} (\mathcal{SP3}) : \quad & \underset{\boldsymbol{\alpha}}{\text{Minimize}} \quad \sum_{k \in \mathcal{K}} T_k^{\text{Tot}} & (22a) \\ & \text{s.t.} \quad (8b), (8d). \end{aligned}$$

Due to the NP-hardness of ($\mathcal{SP3}$), we propose a greedy heuristic-based approach to efficiently approximate the optimal solution. First, we rewrite the objective in (22a) as $\sum_k (T_k^{\text{Loc}} + \alpha_k \Delta T_k)$, where $\Delta T_k = T_k^{\text{Tra}} + T_k^{\text{Off}} - T_k^{\text{Loc}}$ represents the latency gain from offloading compared to local processing. Next, we sort tasks in ascending order of ΔT_k , and set $\alpha_k = 1$ for those tasks with the most negative ΔT_k values, until the resource constraint (8b) is satisfied.

D. Overall Algorithm

Algorithm 1 summarizes the proposed AO-SCA method, which alternately solves subproblems ($\mathcal{SP1}$)–($\mathcal{SP3}$) to address the joint optimization in (\mathcal{P}). The algorithm follows an AO scheme in which each subproblem is solved optimally at every iteration. Since the overall objective is non-increasing and bounded below by zero, convergence is guaranteed. We now analyze the computational complexity. Sub-problem 1 is solved iteratively via SCA, with each convex approximation ($\mathcal{SP1.r}$) handled by an interior-point solver. This incurs a complexity of $\mathcal{O}_{\mathcal{SP1}}(R_{\text{SCA}} K^{3.5})$, with R_{SCA} denoting the number of SCA iterations. Sub-problem 2 admits a closed-form solution via KKT conditions, leading to a linear complexity of $\mathcal{O}_{\mathcal{SP2}}(K)$. Sub-problem 3 applies a greedy rounding procedure after sorting the tasks by ΔT_k , yielding $\mathcal{O}_{\mathcal{SP3}}(K \log K)$. Let R_{AO} be the number of AO iterations; then, the overall complexity is $\mathcal{O}(R_{\text{AO}}(R_{\text{SCA}} K^{3.5} + K \log K))$.

IV. SIMULATION RESULTS

We evaluate the proposed AO-SCA algorithm under a 3GPP small-cell channel model with Rayleigh fading and path loss $L(d) = 30.6 + 36.7 \log_{10}(d) + \mu$ (dB), where d (in meters) is the transmission distance and $\mu \sim \mathcal{N}(0, 8 \text{ dB})$ represents the log-normal shadow fading component [16]. We set $K = 10$, $\sigma^2 = -110$ dBm, $f_t = 2.45$ GHz (ARMv8), $f_0 = 168$ MHz (ARM Cortex-M4), and $B = 500$ MHz, unless otherwise specified. The PQES and EVE are located at (0 m, 0 m) and (50 m, 0 m), respectively, and the RCDs are randomly placed within a 50 m radius centered at the PQES. The maximum channel estimation error ϵ is set to 10% of the corresponding path loss, and the AO-SCA stopping threshold is $\delta_{\text{AO}} = 10^{-6}$. All results are averaged over 5000 Monte Carlo runs. Each RCD's data size, d_k , follows a uniform distribution $d_k \sim \text{U}[10, 50]$ KB. The corresponding CPU cycles per bit, c_k , are randomly assigned from Table I, reflecting each RCD may employ a different PQC algorithm and require a distinct security level [6]–[8]. We compare the performance of our proposed AO-SCA algorithm (*Proposed approach*) against three baselines (BL), along with a traditional no-EVE setup that serves as an upper-bound (UB) reference:

BL I - Constant transmission power (CTP): All RCDs transmit at the maximum power, $p_k = p^{\text{MAX}}$, $\forall k \in \mathcal{K}$; Computing capacity allocation and offloading decisions are still optimized using Algorithm 1.

BL II - Uniform computing capacity (UCC): The PQES divides its computing resources uniformly among all associated users; The optimal RCDs' transmit power and the binary decision variables are jointly optimized using Algorithm 1.

BL III - Full local computing (FLC): Each RCD processes cryptographic tasks locally, i.e., $\alpha_k = 0$, $\forall k \in \mathcal{K}$.

UB - No EVE: Setting $g_k = 0$, $\forall k \in \mathcal{K}$ in problem (\mathcal{P}) yields an upper bound on performance without considering EVE.

Fig. 2 illustrates the impact of the data size per RCD on the total latency for the proposed approach and the baseline schemes. As the data size d_k increases, all schemes exhibit a monotonic increase in total latency due to higher communication and computation demands. The proposed approach consistently achieves the lowest latency across all data sizes, demonstrating its effectiveness in balancing offloading decisions, transmit power control, and computing resource allocation. Baseline I (CTP), which uses a fixed transmit power, performs approximately 60% worse than the proposed method due to its lack of adaptability in transmission control. Baseline II (UCC), which applies uniform computing capacity allocation (while still optimizing the RCDs' transmit power and binary decision variables via Algorithm 1), delivers moderate performance, about 10% worse than the proposed scheme, but still falls short. Baseline III (FLC), which assumes full local computing, incurs the highest latency, emphasizing the importance of edge offloading in PQEC scenarios involving resource-constrained devices. Even when compared with the upper bound (i.e., the No EVE scenario), the proposed method exhibits only a minor performance gap. This demonstrates that our PLS-assisted offloading framework achieves robust edge-domain security at virtually no additional performance cost and underscores the effectiveness of the co-designed computation offloading and PLS strategy in mitigating eavesdropping overhead.

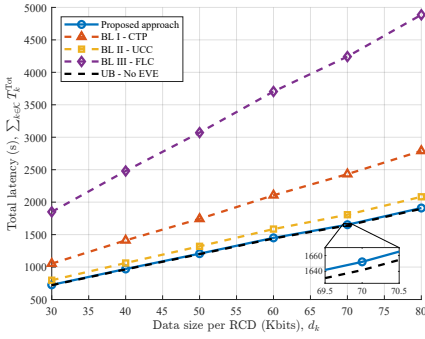


Fig. 2. System total latency versus transmit data size per RCD, d_k .

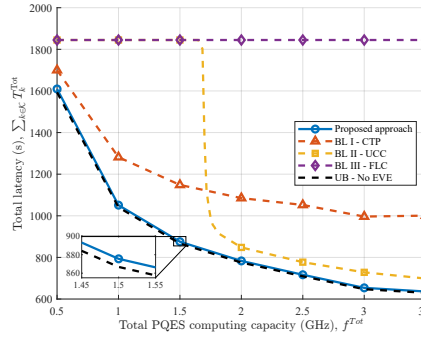


Fig. 3. System total latency versus the PQES computing capacity, f^{Tot} .

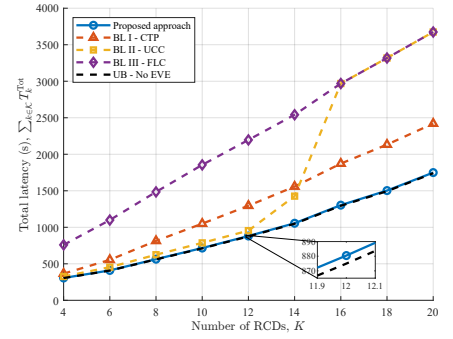


Fig. 4. System total latency versus versus the number of RCDs, K .

Next, Fig. 3 presents total latency as a function of the PQES's computing capacity f^{Tot} . As expected, increasing f^{Tot} significantly reduces latency for offloading schemes, with the proposed approach outperforming all baselines at every capacity level. Although baseline I (CTP) sees reduced latency as f^{Tot} increases, its performance is still markedly inferior due to fixed power settings. Baseline II (UCC) exhibits a sharp latency drop around 1.7 GHz as it benefits from the additional computing resources; however, its uniform resource allocation still results in suboptimal performance. These results underscore the performance advantage of the proposed approach, which is particularly evident in lower computing capacities, where intelligent resource allocation becomes crucial. Meanwhile, Baseline III (FLC), which relies solely on local computing, shows no latency improvement with increases in f^{Tot} , highlighting its disadvantage without edge computing support. Notably, the proposed approach remains close to upper-bound across varying f^{Tot} , demonstrating that the PLS-assisted strategy effectively mitigates the impact of EVE and preserves near-optimal performance.

Finally, Fig. 4 illustrates how the total latency scales with the number of RCDs K . As the network grows, all schemes experience increased latency due to higher communication and computation demands. Nonetheless, the proposed approach consistently achieves the lowest latency, with its advantage becoming more pronounced at larger values of k , where dynamic joint allocation of transmit power and edge computing resources is critical. Baseline I (CTP) and II (UCC) both display rising trends, but their fixed strategies in power or computing allocation lead to suboptimal performance under high device counts. In particular, Baseline II exhibits a sudden latency spike after $K = 14$, highlighting bottlenecks resulting from uniform capacity allocation; as the number of devices grows, dynamic allocation becomes essential. Baseline III (FLC), relying solely on local computing, performs worst, demonstrating poor scalability and high latency, underscoring the limitations of local processing in large networks. Moreover, the proposed approach remains close to the upper bound even as K grows, underscoring its ability to effectively handle adversarial threats through PLS-assisted offloading.

V. CONCLUSION

In this paper, we proposed a novel co-design strategy that integrates PLS techniques and computation offloading to address the challenges of implementing PQC in IoT environments. By jointly optimizing device transmit power, PQES computing capacity allocation, and offloading decisions, our

AO-SCA algorithm tackles the non-convex, NP-hard formulation through alternating optimization and successive convex approximation. Numerical results confirm that the proposed method substantially reduces latency and improves security compared to baseline schemes, even under channel uncertainty. Furthermore, our proposed approach achieves performance nearly identical to the upper-bound (No EVE) scenario, confirming that robust edge-domain security can be attained with our framework at a negligible additional cost.

REFERENCES

- [1] E. Illi and *et al.*, "Physical layer security for authentication, confidentiality, and malicious node detection: A paradigm shift in securing IoT networks," *IEEE Commun. Surv. Tutor.*, vol. 26, no. 1, pp. 347–388, 2024.
- [2] C. Patrick and P. Schaumont, "The role of energy in the lightweight cryptographic profile," in *Proc. NIST Lightweight Cryptogr. Workshop*, 2016, pp. 1–16.
- [3] P. W. Shor, "Algorithms for quantum computation: discrete logarithms and factoring," in *Proc. IEEE 35th Annu. Symp. Found. Comput. Sci.*, 1994, pp. 124–134.
- [4] NIST. (2025) Post-quantum cryptography — CSRC. NIST Computer Security Resource Center.
- [5] —. (2023, Aug) Three draft FIPS for post-quantum cryptography. NIST Computer Security Resource Center.
- [6] M. J. Kannwischer and *et al.*, "pqm4: Testing and benchmarking NIST PQC on ARM Cortex-M4," *IACR Cryptol. ePrint Arch.*, vol. 2019, no. 844, 2019.
- [7] R. a. *et al.* Avanzi, "Crystals-kyber algorithm specifications and supporting documentation," *NIST PQC Round*, vol. 2, no. 4, pp. 1–43, 2019.
- [8] wolfSSL Inc. (2024) wolfssl benchmarks. wolfSSL. [Online]. Available: <https://wolfssl.jp/docs-3/benchmarks/>
- [9] N. N. Minhas and K. Mansoor, "Edge-computing-based scheme for post-quantum IoT security for e-health," *IEEE Internet Things J.*, vol. 11, no. 19, pp. 31 331–31 337, 2024.
- [10] S. Ebrahimi, S. Bayat, and H. Mosanaei-Boorani, "Post-quantum crypto-processors optimized for edge and resource-constrained devices in IoT," *IEEE Internet Things J.*, vol. 6, no. 3, pp. 5500–5507, 2019.
- [11] J. Zhang, B. Chen, Y. Zhao, X. Cheng, and F. Hu, "Data security and privacy-preserving in edge computing paradigm: Survey and open issues," *IEEE Access*, vol. 6, pp. 18 209–18 237, 2018.
- [12] A. D. Wyner, "The wire-tap channel," *Bell Syst. Tech. J.*, vol. 54, no. 8, pp. 1355–1387, 1975.
- [13] H. Amirara, M. Mirmohseni, A. Elzanaty, Y. Ma, and R. Tafazolli, "A physical layer security framework for IRS-assisted integrated sensing and semantic communication systems," *arXiv preprint arXiv:2410.06208*, 2025.
- [14] Y. Dai, D. Xu, S. Maharjan, and Y. Zhang, "Joint computation offloading and user association in multi-task mobile edge computing," *IEEE Trans. Veh. Technol.*, vol. 67, no. 12, pp. 12 313–12 325, 2018.
- [15] M. R. A. Khandaker, K.-K. Wong, Y. Zhang, and Z. Zheng, "Probabilistically robust SWIPT for secrecy MISOME systems," *IEEE Trans. Inf. Forensics Secur.*, vol. 12, no. 1, pp. 211–226, 2017.
- [16] J. Ikuno, M. Wrulich, and M. Rupp, "3GPP TR 36.814 V9.0.0: Further advancements for E-UTRA physical layer aspects," 3GPP, Technical Report 3GPP TR 36.814 V9.0.0, 2010.